# Ultrafast laser-induced spin-lattice dynamics in the van der Waals antiferromagnet $CoPS_3$

Khusyainov, D.; Gareev, T.; Radovskaia, V.; Sampathkumar, K.; Acharya, S.; Šiškins, M.; Mañas-Valero, S.; Ivanov, B. A.; Coronado, E.; More Authors

**DOI**
10.1063/5.0146128

**Publication date**
2023

**Document Version**
Final published version

**Published in**
APL Materials

APL Materials

RESEARCH ARTICLE | JULY 05 2023

# Ultrafast laser-induced spin–lattice dynamics in the van der Waals antiferromagnet $CoPS_3$

**Special Collection:** Emerging Materials in Antiferromagnetic Spintronics

D. Khusyainov ; T. Gareev ; V. Radovskaia ; K. Sampathkumar ; S. Acharya ; M. Šiškins ; S. Mañas-Valero ; B. A. Ivanov ; E. Coronado ; Th. Rasing ; A. V. Kimel ; D. Afanasiev



*APL Mater* 11, 071104 (2023)
https://doi.org/10.1063/5.0146128

# Ultrafast laser-induced spin–lattice dynamics in the van der Waals antiferromagnet $CoPS_3$

Cite as: APL Mater. 11, 071104 (2023); doi: 10.1063/5.0146128
Submitted: 10 February 2023 • Accepted: 12 June 2023 •
Published Online: 5 July 2023



D. Khusyainov,[1,a)] T. Gareev,[1] V. Radovskaia,[1] K. Sampathkumar,[1,2] S. Acharya,[3] M. Šiškins,[4] S. Mañas-Valero,[5] B. A. Ivanov,[1,6] E. Coronado,[5] Th. Rasing,[1] A. V. Kimel,[1] and D. Afanasiev[1]

## AFFILIATIONS

[1] Radboud University, Institute for Molecules and Materials, 6525 AJ Nijmegen, The Netherlands
[2] Central European Institute of Technology, Brno University of Technology, Purkyňova 648/125, Brno 62100, Czech Republic
[3] National Renewable Energy Laboratory, Golden, Colorado 80401, USA
[4] Kavli Institute of Nanoscience, Delft University of Technology, Lorentzweg 1, 2628 CJ Delft, The Netherlands
[5] Instituto de Ciencia Molecular (ICMol), Universitat de València, c/Catedrático José Beltrán 2, 46980 Paterna, Spain
[6] Institute of Magnetism, NAS and MES of Ukraine, 36b Vernadsky Blvd., Kiev 03142, Ukraine

**Note:** This paper is part of the Special Topic on Emerging Materials in Antiferromagnetic Spintronics.
[a)] **Author to whom correspondence should be addressed:** dinar.khusyainov@ru.nl

## ABSTRACT

$CoPS_3$ stands out in the family of the van der Waals antiferromagnets $XPS_3$ (X = Mn, Ni, Fe, and Co) due to the unquenched orbital momentum of the magnetic $Co^{2+}$ ions, which is known to facilitate the coupling of spins to both electromagnetic waves and lattice vibrations. Here, using a time-resolved magneto-optical pump–probe technique, we experimentally study the ultrafast laser-induced dynamics of mutually correlated spins and lattice. It is shown that a femtosecond laser pulse acts as an ultrafast heater and, thus, results in the melting of the antiferromagnetic order. At the same time, the resonant pumping of the $^4T_{1g} \rightarrow {}^4T_{2g}$ electronic transition in $Co^{2+}$ ions effectively changes their orbital momentum, giving rise to a mechanical force that moves the ions in the direction parallel to the orientation of their spins, thus generating a coherent $B_g$ phonon mode at the frequency of about 4.7 THz.





## INTRODUCTION

Since the seminal discovery of ultrafast demagnetization in Ni,[1] the ultrafast manipulation of magnetism with ultrashort pulses of light has evolved into a fascinating research topic of nonequilibrium magnetism, with examples ranging from excitation of collective magnetic modes[2–6] to light-driven magnetic phase transitions[7–9] and switching of spin orientation.[10–12] The recent resurgence of interest in two-dimensional (2D) van der Waals (vdW) materials hosting intrinsic long-range magnetic orders has offered a novel playground for investigating these phenomena in systems where the interplay between structural and magnetic orders plays a pivotal role.[13–17] Understanding the nonequilibrium dynamics in vdW magnets particularly promises to provide important insights into the fundamental physics of spin–lattice interactions and spin relaxation in ultimately thin magnets. Moreover, the inherently strong light–matter interactions, typical of vdW materials,[13,18–24] open up exciting possibilities for efficient manipulation of magnetism on the ultrafast timescale, promising novel energy-efficient data processing devices for future spintronics and magnonics applications.[25,26]

Among the various vdW magnets, transition metal thiophosphates, $XPS_3$ ($X$ = Fe, Ni, Mn, and Co), form a unique class of 2D antiferromagnets (AFMs) with intralayer AFM order on a honeycomb lattice. In addition to the 2D AFM order, previous studies of $XPS_3$ have uncovered strongly coupled spin and charge orders,[27,28] highly anisotropic excitons,[29] magneto-electric coupling,[30,31] signatures of the Berezinskii–Kosterlitz–Thouless (BKT) transition,[32] and strong electron correlations.[33,34] The family has also recently attracted a lot of attention for its ultrafast control of magnetism. In particular, it has been shown that a sudden perturbation of electron

orbital momentum via resonant pumping of specific electronic transitions opens up new ways to control spins and lattice at an ultrafast timescale.[19,20,34,35] $CoPS_3$ stands out in the $XPS_3$ family due to the $Co^{2+}$ ions, characterized by the large spin and unquenched orbital momentum. The presence of such ions in magnetic materials usually results in a strong coupling of the spins to the lattice,[36,37] large magnetocrystalline anisotropy,[38] high frequencies of magnetic resonance,[39] and strong photomagnetic effects.[11,36,37] Furthermore, it has (not sure about "been")recently suggested that the high-spin $d^7$ configuration of $Co^{2+}$-based compounds may host a dominant Kitaev interaction.[40–42] However, despite intense studies of the $XPS_3$ family, the ultrafast optical control of magnetism and lattice in $CoPS_3$ remains unexplored.

Here, we address these shortcomings by first introducing optical magnetic linear dichroism (MLD) as an efficient means to probe the AFM order in $CoPS_3$ and then employing time-resolved magneto-optical pump–probe spectroscopy to detect the ultrafast light-induced dynamics of spins and lattice in this AFM compound. Comparison of the results with earlier studies for $MnPS_3$ and $FePS_3$ reveals that the presence of the large unquenched orbital momentum in $CoPS_3$ results in a substantially higher MLD and much faster laser-induced melting of the spin order. Moreover, the unquenched momentum leads to exceptionally strong spin–lattice coupling and provides an opportunity for highly efficient optical control of the lattice dynamics by the selective pumping of specific orbital transitions in magnetic $Co^{2+}$ ions.

## SAMPLE AND EXPERIMENTAL PROCEDURE

$CoPS_3$ is a layered van der Waals AFM, characterized by a weak coupling between the adjacent crystal and magnetic layers, which can be viewed approximately as a quasi-2D antiferromagnet.[43] The intralayer spin ordering below $T_N$ = 120 K results in the formation of ferromagnetic "zigzag" chains along the $a$-axis, while the adjacent chains in the direction of the $b$-axis are AFM coupled (see Fig. 1(a). Introducing individual magnetizations of the adjacent chains as $\mathbf{M}_1$ and $\mathbf{M}_2$, the AFM order in $CoPS_3$ can be naturally characterized by a Néel vector $\mathbf{L}$, such that $\mathbf{L} = \mathbf{M}_2 - \mathbf{M}_1$. Inelastic neutron scattering shows that $CoPS_3$ has sizable easy-axis single-ion anisotropy, which defines the orientation of the spins and the resultant Néel vector along the crystallographic $a$-axis.[40] The formation of spin chains, combined with a strong spin–lattice interaction of $Co^{2+}$ ions, leads to a reduction of the crystal symmetry, such that the point group of a single $CoPS_3$ layer changes from $D_{3d}$ to $C_{2h}$.[16] Above $T_N$ in the paramagnetic (PM) phase, the crystal lattice is characterized by a six-fold rotational symmetry. Below $T_N$, the ordering of spins in chains leads to a compression of $a$ and an elongation of $b$ lattice parameters, effectively elongating the hexagons formed by the $Co^{2+}$ ions in the direction perpendicular to the spin chains. The structural changes that accompany the magnetic transition strongly affect the vibrational (phonon) spectrum of $CoPS_3$. Recent Raman studies show that upon spin ordering, several otherwise double degenerate $E_g$ phonon modes lose their degeneracy and split into a pair of nondegenerate $A_g$ and $B_g$ ones, of which the frequencies demonstrate an anomalous behavior below $T_N$.[16]

To be able to employ an all-optical pump-and-probe technique for studies of ultrafast magnetism in $CoPS_3$, one must find an efficient method of the optical detection of spin order in the AFM phase. Earlier, it was reported that several $XPS_3$ materials possess a large magnetic linear dichroism (MLD) in the AFM phase.[13,44] Moreover, according to Refs. 13, the strength of the dichroism seems to scale with the orbital moment of the magnetic ion. The MLD is the smallest in $MnPS_3$, where the orbital momentum of the magnetic $Mn^{2+}$ ions is quenched, and the largest in $FePS_3$, where the orbital momentum of $Fe^{2+}$ is known to be non-zero. To reveal the strength of this magneto-optical effect in $CoPS_3$, with an even larger orbital momentum associated with the $Co^{2+}$ ions, we measured the transmittance of linearly polarized probe light at a photon energy of 1.55 eV as a function of the angle $\vartheta$ between the electric field of light and the $a$-axis of the crystal. Figures 1(b) and 1(c) show the polarization dependencies below ($T$ = 7 K) and above ($T$ = 300 K) the $T_N$. It is seen that the normalized transmittance is strongly anisotropic if the material is in the AFM state. Measuring the difference between the intensities $I_a$ and $I_b$ of the transmitted light polarized along the $a$- and the $b$-axes, respectively, we define MLD as

$$\alpha_{MLD} = \frac{(I_a - I_b)}{(I_a + I_b)} \cdot 100\%. \quad (1)$$

Although MLD, in general, strongly depends on the probe photon energy, already in our experiment its value reaches 30%. This is almost an order of magnitude larger than the largest MLD reported for $FePS_3$.[13] To define the origin of the MLD in $CoPS_3$, we studied the effect as a function of the probe photon energy. As shown in the supplementary material Fig. S1, two well-pronounced MLD bands appear with the maxima centered at the photon energies of about 1.69 and 2.34 eV. These energies closely match the energies of the so-called $d$–$d$ transitions of $Co^{2+}$ ions that are responsible for the change of the orbital state of the magnetic ion.[45] This observation, thus, indicates that the $d$–$d$ transitions are the origin of MLD in $CoPS_3$, in agreement with previous studies.[13,19,20,35]

Figure 1(d) shows MLD in $CoPS_3$ as a function of temperature $T$. It is seen that $\alpha_{MLD}$ reduces significantly when approaching $T_N$ from below. To quantify the critical behavior of $\alpha_{MLD}$, we fitted the temperature dependence of $\alpha_{MLD}$ in the AFM phase using a power law $\alpha_{MLD} \propto |T_N - T|^{2\beta}$. The results, shown in Fig. 1(d), yield $2\beta = 0.60 \pm 0.01$. This value agrees well with the critical exponent characterizing a temperature scaling of the decay in the intensity of the neutron Bragg diffraction peak from the underlying AFM order in $CoPS_3$ which was found to be $2\beta = 0.60$.[43] As the Bragg intensity scales with the Néel order as $L^2$, its comparison with our results suggests that $\alpha_{MLD}$ also scales as $L^2$. In theory, MLD should be quadratic concerning $\mathbf{L}$, but experimentally, this is not always the case, especially in AFMs with strong piezomagnetism.[46] At the same time, MLD is known to be one of the most universal effects to probe the AFM order using light in a broad spectral range, including THz,[47] visible,[48,49] and x-rays.[50] Yielding $\beta \approx 0.30$ for the critical exponent characterizing the temperature dependence of the AFM order parameter, our results further confirm that the spin order in $CoPS_3$ is best described by the 3D Ising model.[51] Note, the dichroism, as defined in this work, does not depend on the sample thickness and, thus, can be potentially employed to probe AFM spin order in $CoPS_3$ down to a single layer. At the same time, we observed that in the finite size $CoPS_3$ samples studied in our experiments, the linear dichroism does not completely vanish above $T_N$;

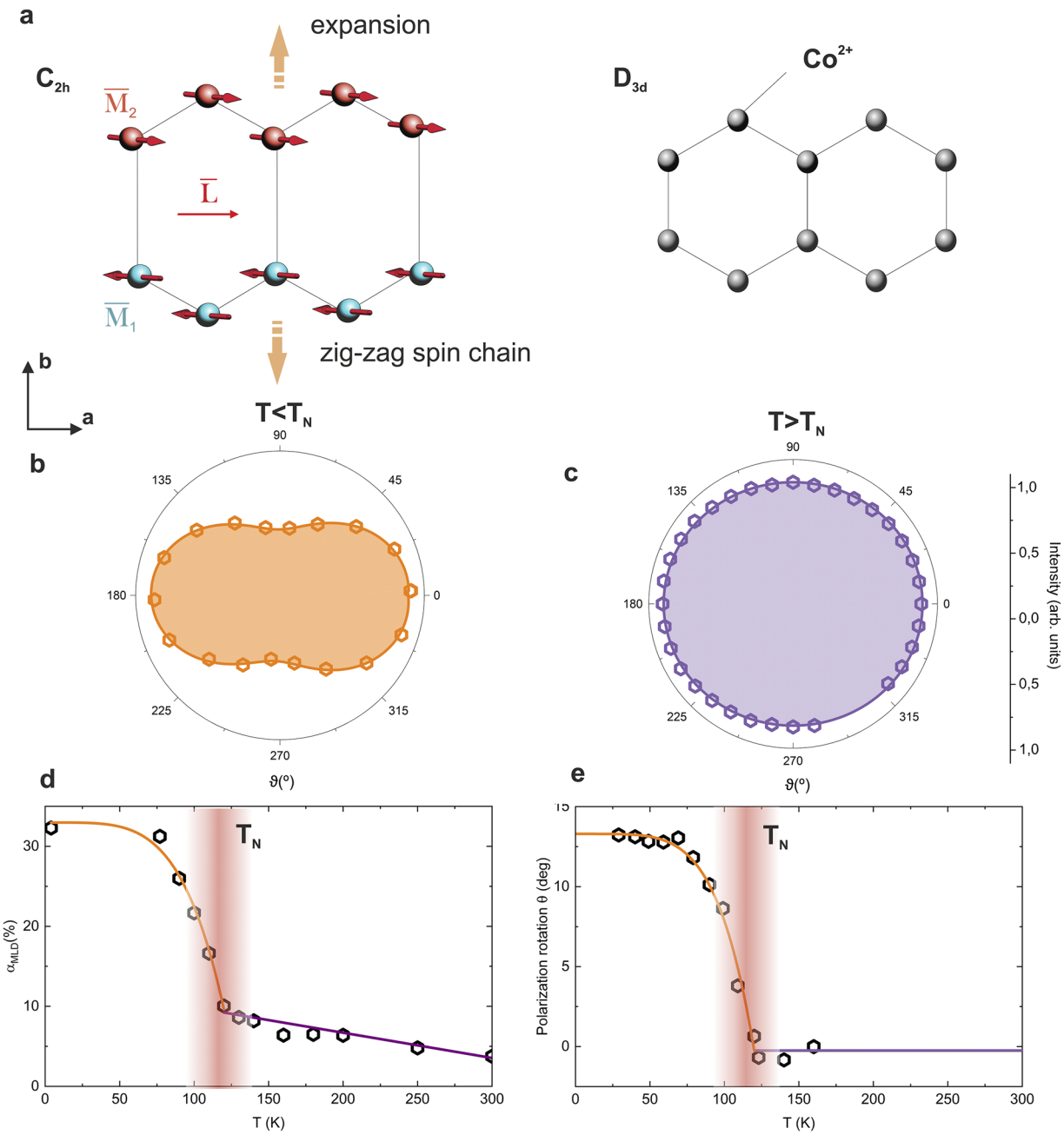


**FIG. 1.** (a) Schematics of the AFM spin and crystal structure of $CoPS_3$ in the antiferromagnetic and paramagnetic phases. (b), (c) The normalized transmission of light as a function of linear polarization angle $\vartheta$ measured below and above $T_N$, respectively. The angle $\vartheta = 0$ corresponds to the orientation of the polarization plane along the a-axis. (d) Magnetic linear dichroism ($\alpha_{MLD}$) of $CoPS_3$ measured as a function of temperature. The solid line is a guide to the eye. (e) Rotation of the light polarization plane $\theta$ as a function of temperature. The solid line is a guide to the eye. The photon energy of the probe light is 1.55 eV.

see Fig. 1(d). This is because the ideal six-fold rotational symmetry of the honeycomb lattice, present in a single-layer form, vanishes in bulk crystals due to the displacement of the stacked layers along the *a*-axis.[31]

In our experiments, to probe the anisotropy of the optical properties induced by the spin order, we employ the fact that if the polarization of the incoming light does not orient along and/or perpendicularly to the Néel vector (the *a*- and *b*-axes, respectively), the

MLD will result in rotation of the polarization plane for light propagating through the sample. In our case, the light, initially polarized at 45° with respect to both the *a*- and *b*-axes, upon propagation through a 4 $\mu$m thick sample experiences a net polarization rotation for an angle reaching about 13° [Fig. 1(e)]. We note that, although the value of the angle is large, it is by far less than expected for an MLD as large as 30%. This difference can be explained by the fact that according to the Kramers–Kronig relations,[52,53] linear dichroism is always accompanied by linear birefringence. The latter can modify the polarization state of light from linear to elliptical and even circular and, thus, substantially hampers the measurements of the polarization rotation.[54]

To study the light-induced ultrafast dynamics of spins and lattice in $CoPS_3$, we carried out an all-optical pump–probe experiment; see Fig. 2(a). To excite the dynamics, we employed ultrashort (~50 fs) linearly polarized pulses of light with the photon energy *hv* tunable in a range from 0.7 to 2.5 eV. This energy range covers the vast majority of the orbital *d*–*d* transitions in $Co^{2+}$ ions.[45] To probe the light-driven spin dynamics, we relied on measuring the transient polarization rotation $\Delta\theta$ providing, as we have already shown, access to the Néel order. The polarization rotation was also employed to detect the lattice vibrations (phonons), of which the dynamics are intrinsically highly anisotropic and, thus, contribute to the linear birefringence.[18,55] Figure 2(b) shows an example of the light-induced dynamics triggered by the pump pulse at a temperature of $T$ = 77 K when the sample is in the AFM phase. It is seen that, after the excitation, the signal of the transient rotation $\Delta\theta$ suddenly drops, indicating a suppression of the AFM order. Note, that the suppression does not occur instantaneously within the duration of the pump pulse but rather proceeds on a longer timescale $\tau_s$ of about 1.5 ps [Fig. 2(b)]. The quenching of the AFM order is concomitant with a set of coherent high-frequency phonon oscillations featuring frequencies from 3 to 10 THz and dominated by a phonon mode at 4.74 THz; see the inset in Fig. 2(b) and the supplementary material in Fig. S2.

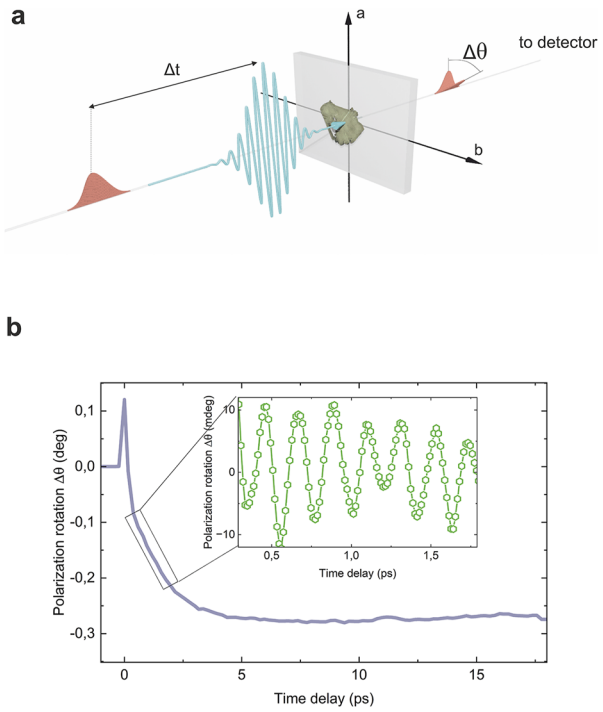


**FIG. 2.** (a) Schematics of the time-resolved magneto-optical pump–probe experiment in $CoPS_3$. The pump pulse (blue) is delayed with respect to the probe pulse by a variable time delay $\Delta t$. (b) Time-resolved rotation of the probe pulse polarization plane exemplifying pump-induced quenching of the AFM order. The inset shows zoom-in of the background-free dynamics of the coherent $B_g$ phonon mode. The sample temperature is set to 77 K.

## SPIN DYNAMICS

Figure 3(a) shows the dynamics of the pump-induced polarization rotation $\Delta\theta$, demonstrating the evolution of the light-induced quenching as a function of the temperature $T$. We fit the time-resolved traces to a single exponential function from which we extract amplitude and quenching time; see the supplementary material S3. It is seen [Fig. 3(b)] that upon approaching $T_N$ the amplitude of the quenching is gradually growing and peaks right below $T_N$. Above $T_N$, no significant light-induced magnetic dynamics is seen; the small residual signal is likely of non-magnetic origin and caused by pump-induced changes to the electronic part of the dielectric function.[56] The growth of the quenching amplitude is accompanied by the growth of the quenching time $\tau_s$. Upon approaching $T_N$ [Fig. 3(c)], this time increases from 1.6 ps at $T$ = 10 K to a maximum detected time of 5 ps at about $T$ = 118 K. We note that qualitatively similar behavior was also observed when the probing was performed in the reflection geometry; see the supplementary material Fig. S4.

To establish the origin of the AFM quenching, we varied the photon energy of the pump pulse in the range of several *d*–*d* transitions of $Co^{2+}$ ions. We find that the amplitude of the quenching scales with the absorption does not depend on the origin of the optical transition. The quenching is defined by the amount of heat deposited into $CoPS_3$ by a laser pulse. The origin of the laser-induced quenching of AFM order is, thus, similar to that reported earlier for other materials from the $XPS_3$ family.[18] Although laser-induced demagnetization is often described using a three-temperature 3*T*-model,[1] $CoPS_3$ lacks free electrons and the model is not adequate in this case. Instead, the quenching of the AFM order in $CoPS_3$ can be described by a two-temperature 2*T* model, where the pump photons increase the potential energy of the excited electrons without making them hot. Upon non-radiative recombination of the excited electrons, the latter promptly (<1 ps) transfer the gained photon energy to the lattice.[57] The subsequent heat exchange via spin–lattice interaction leads to an increase in the effective spin temperature and consequently to the melting of the spin order.[58] This mechanism can explain a substantial increase in the magnitude of the quenching as the temperature approaches $T_N$. Indeed, at higher temperatures, the derivative of the Néel order parameter $L$ with respect to the temperature increases, and the spins become more susceptible to temperature variations; see Fig. 1(d). Remarkably, not only the amplitude of the quenching goes up, but the quenching time $\tau_s$ also experiences a substantial increase in the vicinity of $T_N$. Such a critical slowing down of the transient spin dynamics induced by

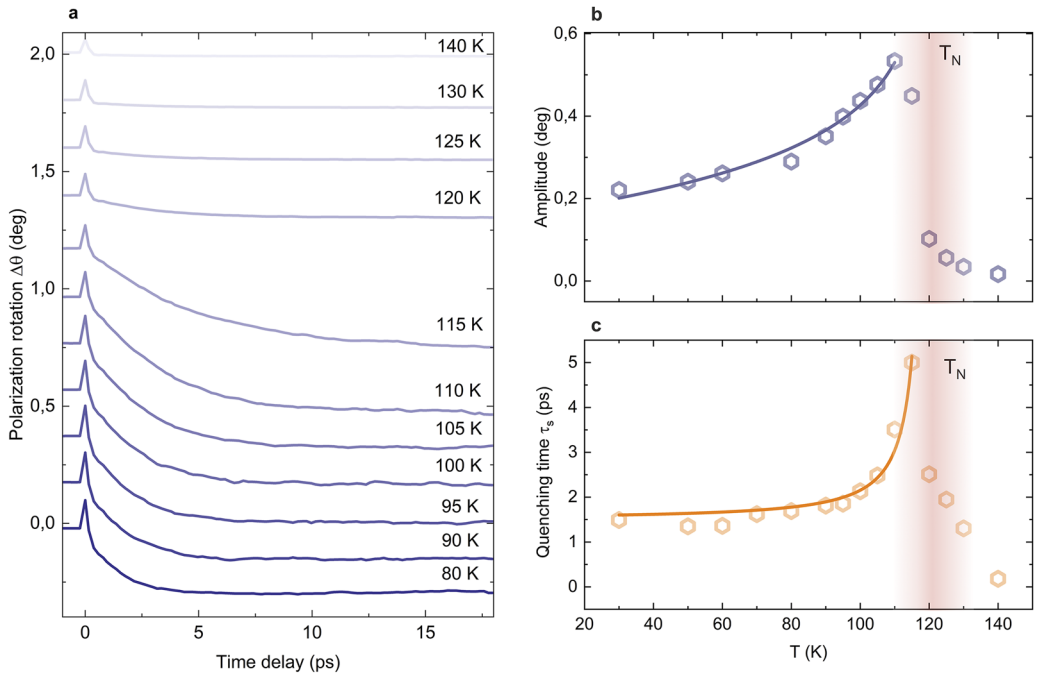


**FIG. 3.** Ultrafast light-induced quenching of the Néel order in $CoPS_3$ (a) Time-resolved rotation of the probe polarization $\Delta\theta$ showing pump-induced quenching of the AFM order for various temperatures across $T_N$. The pump photon energy is 0.9 eV. (b) Amplitude of the quenching as a function of temperature $T$. (c) Quenching time as a function of $T$.

light is seen in many AFM compounds, including in recently published results on $MnPS_3$ and $FePS_3$.[19,35] It has been shown[18] that in magnetic insulators the rate of the spin–lattice coupling defining $\tau_s$ scales with the spin-specific heat $C_s$, such that $\tau_s = C_s/g_{sl}$, where $g_{sl}$ is the spin–lattice relaxation rate representing the strength of the spin–lattice interaction. As the heat capacity near the Néel temperature is expected to diverge, assuming a weak temperature dependence of $g_{sl}$ near $T_N$, the characteristic time $\tau_s$ is expected to follow the divergence of $C_s$. Indeed, our experiment shows that $\tau_s \propto |T_N - T|^{-\alpha}$ with a critical exponent $\alpha \sim 0.1$. Remarkably, this value closely matches the theoretical one of $\alpha = 0.1$ characterizing the critical scaling of the heat capacity in the 3D Ising model.[51,59]

We would like to emphasize that the characteristic time for the quenching of the AFM order in $CoPS_3$ ($\tau_s = 2$ ps) is much shorter than the one reported for other $XPS_3$ compounds and $MnPS_3$, in particular ($\tau_s = 30$ ps).[19] It is well known that the heat capacity $C_s$ scales with the strength of the exchange interaction, which is proportional to the Néel temperature. As $CoPS_3$ and $MnPS_3$ are characterized by similar values of $T_N$, the difference in the quenching time can only be explained by a difference in the magnitude of the spin–lattice relaxation rate $g_{sl}$. Using the available data for the specific heat capacity,[16,60] we estimate $g_{sl}$ to be about $1 \times 10^{14}$ $Wm^{-3}$ $K^{-1}$ and $5 \times 10^{11}$ $Wm^{-3}$ $K^{-1}$ for $CoPS_3$ and $MnPS_3$, respectively. Our experiment, thus, shows that the strength of the coupling can be effectively changed by more than two orders of magnitude by inducing an orbital momentum at the ground state of the magnetic ion. We note that, although the obtained values of the spin–lattice relaxation rates in $CoPS_3$ due to the unquenched momentum of the $Co^{2+}$ ions are high, this is only in comparison with electronically similar materials lacking mobile electrons (dielectrics and semiconductors). In metals, free electrons serve as an additional reservoir of energy that can increase the rate of laser-induced demagnetization by another two orders of magnitude.[61]

## LATTICE DYNAMICS

To further understand the nature and excitation mechanism of the light-driven coherent phonon mode that dominates the $\Delta\theta$ signal, we studied its dynamics as a function of both temperature and photon energy. Figure 4(a) shows the oscillations measured at various $T$. It is seen that the excitation is the most efficient below $T_N$, where both the amplitude and the frequency of the oscillations are strongly dependent on $T$. Using the Fourier transform, we retrieved the frequency and amplitude of the oscillations and plotted them as functions of $T$ in Figs. 4(b) and 4(c), respectively. As the temperature increases, the phonon frequency $f$ softens until it reaches $T_N$, where it stabilizes at $f_0 = 4.64$ THz. Fitting the temperature evolution of the frequency shift $\Delta f = f - f_0$ to a critical law similar to the one used for $\alpha_{MLD}$, we find that their critical exponents closely match each other, thus indicating that $\Delta f$ also follows $L^2$. In accordance with Ref. 16, we assign the oscillations to the $B_g$ phonon mode that involves antiphase motions of the magnetic $Co^{2+}$ ions in the direction parallel to the orientation of their spins [Fig. 5(b)]. The comparison of the temperature behavior of the amplitude of the phonon mode in AFM and PM phases shows that, in PM ($T > T_N$), there

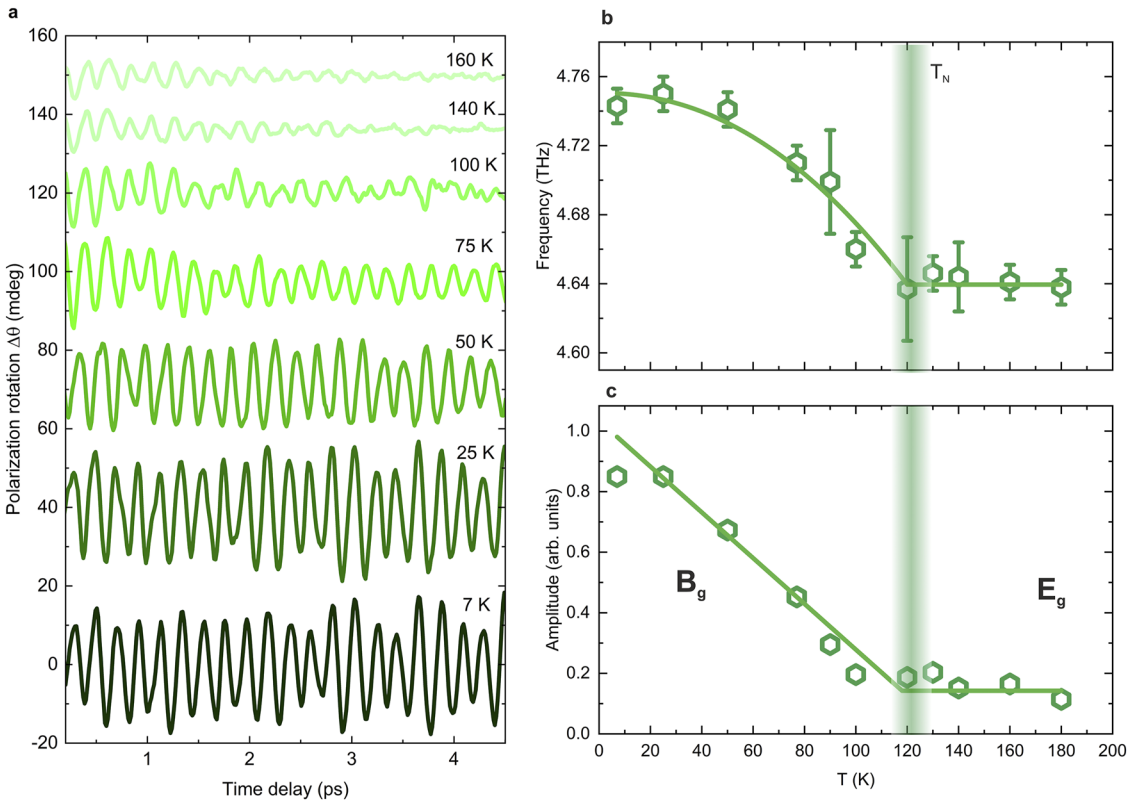


**FIG. 4.** High frequency coherent spin-coupled THz phonon mode in $CoPS_3$. (a) Time-resolved rotation of the probe polarization showing dynamics of the pump-excited coherent phonon plotted for various temperatures across $T_N$. (b) Frequency f of the phonon mode as a function of temperature $T$. (c) Amplitude of the phonon mode as a function of temperature $T$. The solid lines are independent linear fits below and above $T_N$.

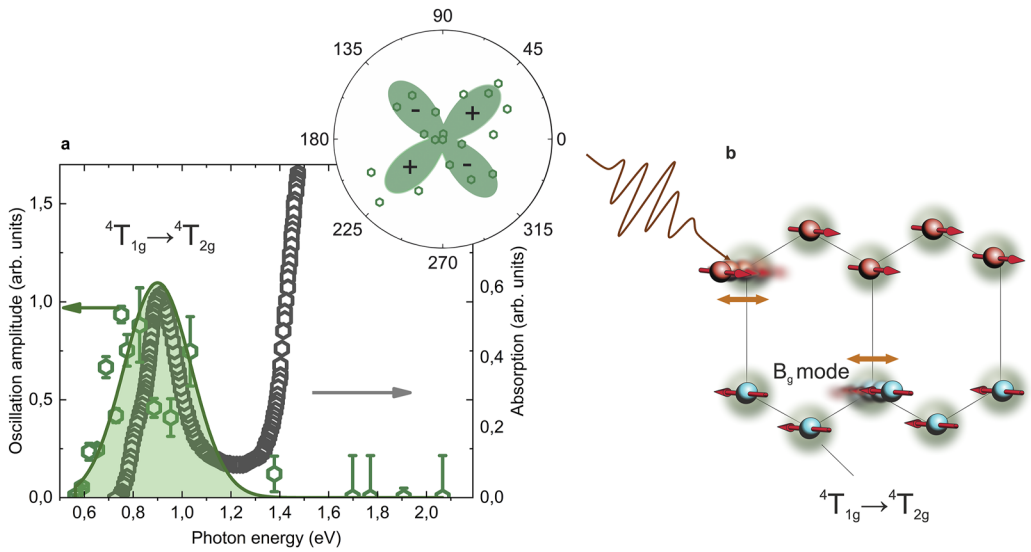


**FIG. 5.** (a) The amplitude of the $B_g$ phonon mode as a function of the pump photon energy (left axis). Optical absorption of $CoPS_3$ in the near IR to the visible range: the absorption line at around 0.9 eV corresponds to the $^4T_{1g} \rightarrow {}^4T_{2g}$ orbital transition (right axis). The data are taken from Ref. 44. The samples temperature is 77 K. Inset: Amplitude of the phonon as a function of the pump polarization angle γ with respect to the a-crystal axis. The signs "+" and "−" indicate the relative phase of the oscillations and correspond to 0° and 180°, respectively. (b) Schematics of the orbital excitation of the $B_g$ phonon, where the blue and red ions are $Co^{2+}$ ions with antiparallel spins.

is no significant temperature dependence, but in AFM ($T \leq T_N$), the amplitude rises linearly as temperature decreases. The rise, concomitant with the onset of the AFM order, clearly indicates that the establishment of the Néel order facilitates the excitation of the lattice dynamics.

Figure 5(a) shows the amplitude of the $B_g$ phonon mode as a function of the pump photon energy $h\nu$. Unlike the light-induced spin quenching, the laser-induced lattice dynamics does not correlate with the absorption coefficient but, instead, is most efficient if the photon energy is in resonance with the $d$–$d$ transition ${}^4T_{1g} \rightarrow {}^4T_{2g}$ in the $Co^{2+}$ ions at 0.87 eV.[45] We have also found that the efficiency of the excitation is strongly dependent on the incoming pump polarization. The inset in Fig. 5(a) shows how the amplitude of the phonon oscillations depends on the angle $\gamma$ the pump polarization plane forms with the $a$-axis along which the spins chains are formed. It is seen that the excitation is most efficient if the pump is polarized at 45° with respect to the spins, while no oscillations are excited if the polarization is oriented either along or perpendicularly.

To explain the unusual temperature behavior of the $B_g$ phonon mode and its excitation mechanism, we first refer to Ref. 62, which demonstrates that in $FePS_3$, also characterized by unquenched angular momentum, the spin–lattice interaction leads to the hybridization of spin and lattice dynamics accompanied by renormalization of their frequencies. The energy of such coupling to the lowest order acquires the following form:

$$\Phi^{sp} = U \cdot Q \cdot lL, \tag{2}$$

where $U$ is a phenomenological coupling parameter, $Q$ is the normal coordinate of the $B_g$ mode, and $l \ll L$ is a component of the Néel vector along the $b$-axis, describing its deviation from the ground state $\mathbf{L} = L\hat{\boldsymbol{a}}$. It is, thus, clear that to enable the spin–lattice coupling in $CoPS_3$, the spins have to be brought out-of-equilibrium. Next, we consider the energy of the light–matter interaction enabling excitation of both the Néel vector $l$ and the $B_g$ phonon mode. The energy describing this interaction reads

$$\Phi^{lm} = (\alpha Q + \beta lL) \cdot E_a E_b, \tag{3}$$

where $E_{a,b}$ are time-dependent electric field components of the pump pulse and $\alpha$ and $\beta$ are phenomenological parameters that describe the strength of the light–matter coupling in $CoPS_3$. It is seen that the pump can be coupled not only to the phonon mode but also to the Néel vector. Remarkably, the efficiency of this coupling is proportional to $E_a E_b \propto \sin 2\gamma$ and, thus, perfectly agrees with the pump polarization dependence of the phonon amplitude; see the inset in Fig. 5(a). In the supplementary material we demonstrate that a sufficiently short pump pulse can impulsively excite coherent dynamics of both $Q$ and $l$ in accordance with a mechanism known as impulsive stimulated Raman scattering (ISRS).[63,64] We also show that the inclusion of the spin–lattice coupling hybridizes their dynamics and may explain the enhancement of the phonon amplitude in the AFM phase. Indeed, the hybridization renormalizes the phonon coordinate $\tilde{Q} = Q + \zeta l$. The parameter $\zeta$ characterizes the degree of the hybridization and is proportional to the product $UL$. Therefore, it may naturally explain the enhancement of the phonon excitation in the AFM phase, where $L \neq 0$. Moreover, the hybridization causes a renormalization of the phonon frequency $\Delta f$ in the AFM phase,

$$\Delta f \propto \zeta^2 \propto (UL)^2, \tag{4}$$

which once again lines up with our experimental findings. We note that although the suggested theory explains experimental findings remarkably well, it still relies on the excitation of the coherent spin dynamics, which is not observed in our experiments. This is rather surprising, as the excitation and magneto-optical detection of the coherent spin dynamics with femtosecond optical pulses have been reported recently in both $MnPS_3$ and $NiPS_3$.[19,20] The analogy with the latter is particularly striking as $NiPS_3$ is magnetically isomorphous to the studied here $CoPS_3$. Future probes of the laser-induced spin dynamics in $CoPS_3$, e.g., time-resolved THz spectroscopy, may help to elucidate this issue.[65] In accordance with these theoretical considerations, the resonance dependence of the amplitude of the phonon mode on the pump photon energy, shown in Fig. 5(a), implies that either both or one of the phenomenological parameters $U$ and $\beta$ is maximized at this photon energy. This implies that, among all possible $d$–$d$ electronic transitions in the range from 0.5 to 2.2 eV, the excitation of the $B_g$ mode is most affected by the ${}^4T_{1g}$ to ${}^4T_{2g}$ transition, which can be seen as a change of the effective orbital momentum of the magnetic $Co^{2+}$ ions; see Fig. 5(b). The corresponding changes to the interionic potential, mediated by the strong spin–lattice coupling, are likely due to the mechanical force that moves the ions in the direction parallel to the orientation of their spins.

## CONCLUSIONS

To conclude, we have shown that in the vdW AFM $CoPS_3$, characterized by a strong spin–lattice coupling, the AFM order can be effectively probed with MLD. Using MLD, we detected the ultrafast dynamics of spins and lattice induced by ultrashort pulses of light. We showed that light can suddenly heat the magnetic system, leading to a substantial loss (~1%) of the spin ordering within nearly a single picosecond. Resonantly pumping $d$–$d$ transitions in magnetic $Co^{2+}$ ions, we effectively change the orbital momentum of $Co^{2+}$ ions and show that this excitation, mediated by the spin–lattice coupling, brings $Co^{2+}$ ions in a coherent motion in the direction of the AFM Néel vector. Our experiments not only elucidate the nature of the ultrafast spin–lattice coupling in 2D vdW AFMs but also lay the ground for future ultrafast pump–probe experiments, particularly those aimed at resonant pumping of infrared-active structural phonon modes.[7,66]

## SUPPLEMENTARY MATERIALS

The supplementary material includes five individual sections. Section I shows the spectral dependence of the MLD in $CoPS_3$. Section II demonstrates the time-resolved traces of the pump-excited coherent phonon modes and their corresponding Fast Fourier Transform (FFT) spectra. Section III describes the fitting procedure for the time-resolved dynamics of the pump-induced quenching of the AFM order. Section IV shows the time-resolved traces of the pump-induced polarization rotation reflection in the

reflection geometry. Section V demonstrates the temperature dependence of the spin–lattice coupling constant $g_{sl}$. The phenomenological theory of the spin–phonon coupling mechanism is described in Sec. VI.

## ACKNOWLEDGMENTS

The authors are grateful to M. Matthiessen, J. R. Hortensius, A. D. Caviglia and M. I. Katsnelson for their fruitful discussions and to S. Semin, K. Saeedi, and C. Berkhout for their technical support. This work was funded by the Netherlands Organization for Scientific Research (NWO), the European Union Horizon 2020 and innovation program under the European Research Council ERC Grant Agreement No. 856538 (3D-MAGiC), the European Union Horizon 2020 innovation program under the Marie Skłodowska-Curie Grant Agreement No. 861300 (COMRAD), the National Research Fund of Ukraine within Project No. 2020.02/026, the Gravitation program of the Dutch Ministry of Education, Culture and Science (OCW) under the research program "Materials for the Quantum Age" (QuMat) registration number 024.005.006, and the ERC (Grant Nos. 1010 78206, ASTRAL). S.M.V. acknowledges the Generalitat Valenciana for the postdoctoral fellow APOSTD-CIAPOS2021/215, and S.A. was supported by the Computational Chemical Sciences program within the Office of Basic Energy Sciences, U.S. Department of Energy under Contract No. DE-AC36-08GO28308.

## AUTHOR DECLARATIONS

### Conflict of Interest

The authors have no conflicts to disclose.

### Author Contributions

**D. Khusyainov**: Data curation (lead); Formal analysis (lead); Investigation (lead); Methodology (lead); Validation (equal); Visualization (equal); Writing – original draft (equal); Writing – review & editing (equal). **T. Gareev**: Data curation (supporting); Formal analysis (supporting); Investigation (supporting); Methodology (supporting); Visualization (supporting). **V. Radovskaia**: Data curation (supporting); Formal analysis (supporting); Investigation (supporting); Methodology (supporting); Visualization (supporting). **K. Sampathkumar**: Data curation (supporting); Formal analysis (supporting); Investigation (supporting); Methodology (supporting); Writing – original draft (supporting); Writing – review & editing (supporting). **S. Acharya**: Conceptualization (supporting); Formal analysis (supporting); Writing – review & editing (supporting). **M. Šiškins**: Conceptualization (supporting); Resources (equal); Writing – review & editing (supporting). **S. Mañas-Valero**: Resources (equal); Writing – review & editing (equal). **B. A. Ivanov**: Conceptualization (equal); Investigation (equal); Methodology (equal); Writing – review & editing (equal). **E. Coronado**: Resources (equal); Supervision (equal). **Th. Rasing**: Funding acquisition (equal); Project administration (equal); Supervision (equal); Writing – original draft (equal); Writing – review & editing (equal). **A. V. Kimel**: Conceptualization (equal); Formal analysis (equal); Funding acquisition (equal); Project administration (equal); Supervision (equal); Validation (equal); Writing – review & editing (equal). **D. Afanasiev**: Conceptualization (lead); Data curation (equal); Formal analysis (equal); Funding acquisition (equal); Investigation (equal); Methodology (equal); Project administration (lead); Resources (equal); Supervision (lead); Validation (equal); Visualization (equal); Writing – original draft (lead); Writing – review & editing (lead).

## DATA AVAILABILITY

The data that support the findings of this study are available from the corresponding author upon reasonable request.

## REFERENCES

[1] E. Beaurepaire, J.-C. Merle, A. Daunois, and J.-Y. Bigot, Phys. Rev. Lett. **76**, 4250 (1996).
[2] A. V. Kimel, A. Kirilyuk, P. A. Usachev, R. V. Pisarev, A. M. Balbashov, and T. Rasing, Nature **435**, 655 (2005).
[3] D. Bossini and T. Rasing, Phys. Scr. **92**, 024002 (2017).
[4] A. M. Kalashnikova, A. V. Kimel, R. V. Pisarev, V. N. Gridnev, A. Kirilyuk, and T. Rasing, Phys. Rev. Lett. **99**, 167205 (2007).
[5] S. Baierl, M. Hohenleutner, T. Kampfrath, A. K. Zvezdin, A. V. Kimel, R. Huber, and R. V. Mikhaylovskiy, Nat. Photonics **10**, 715 (2016).
[6] J. R. Hortensius, D. Afanasiev, M. Matthiesen, R. Leenders, R. Citro, A. V. Kimel, R. V. Mikhaylovskiy, B. A. Ivanov, and A. D. Caviglia, Nat. Phys. **17**, 1001 (2021).
[7] D. Afanasiev, J. R. Hortensius, B. A. Ivanov, A. Sasani, E. Bousquet, Y. M. Blanter, R. V. Mikhaylovskiy, A. V. Kimel, and A. D. Caviglia, Nat. Mater. **20**, 607 (2021).
[8] A. V. Kimel, A. Kirilyuk, A. Tsvetkov, R. V. Pisarev, and T. Rasing, Nature **429**, 850 (2004).
[9] P. Beaud, A. Caviezel, S. O. Mariager, L. Rettig, G. Ingold, C. Dornes, S.-W. Huang, J. A. Johnson, M. Radovic, T. Huber, T. Kubacka, A. Ferrer, H. T. Lemke, M. Chollet, D. Zhu, J. M. Glownia, M. Sikorski, A. Robert, H. Wadati, M. Nakamura, M. Kawasaki, Y. Tokura, S. L. Johnson, and U. Staub, Nat. Mater. **13**, 923 (2014).
[10] C. D. Stanciu, F. Hansteen, A. V. Kimel, A. Kirilyuk, A. Tsukamoto, A. Itoh, and T. Rasing, Phys. Rev. Lett. **99**, 047601 (2007).
[11] A. Stupakiewicz, K. Szerenos, D. Afanasiev, A. Kirilyuk, and A. V. Kimel, Nature **542**, 71 (2017).
[12] A. V. Kimel, A. M. Kalashnikova, A. Pogrebna, and A. K. Zvezdin, Phys. Rep. **852**, 1 (2020).
[13] Q. Zhang, K. Hwangbo, C. Wang, Q. Jiang, J.-H. Chu, H. Wen, D. Xiao, and X. Xu, Nano Lett. **21**, 6938 (2021).
[14] B. H. Zhang, Y. S. Hou, Z. Wang, and R. Q. Wu, Phys. Rev. B **100**, 224427 (2019).
[15] A. Ghosh, M. Palit, S. Maity, V. Dwij, S. Rana, and S. Datta, Phys. Rev. B **103**, 064431 (2021).
[16] Q. Liu, L. Wang, Y. Fu, X. Zhang, L. Huang, H. Su, J. Lin, X. Chen, D. Yu, X. Cui, J.-W. Mei, and J.-F. Dai, Phys. Rev. B **103**, 235411 (2021).
[17] Y.-J. Sun, J.-M. Lai, S.-M. Pang, X.-L. Liu, P.-H. Tan, and J. Zhang, J. Phys. Chem. Lett. **13**, 1533 (2022).
[18] X.-X. Zhang, S. Jiang, J. Lee, C. Lee, K. F. Mak, and J. Shan, Nano Lett. **21**, 5045 (2021).
[19] M. Matthiesen, J. R. Hortensius, S. Mañas-Valero, I. Kapon, D. Dumcenco, E. Giannini, M. Šiškins, B. A. Ivanov, H. S. J. van der Zant, E. Coronado, A. B. Kuzmenko, D. Afanasiev, and A. D. Caviglia, Phys. Rev. Lett. **130**, 076702 (2023).
[20] D. Afanasiev, J. R. Hortensius, M. Matthiesen, S. Mañas-Valero, M. Šiškins, M. Lee, E. Lesne, H. S. J. van der Zant, P. G. Steeneken, B. A. Ivanov, E. Coronado, and A. D. Caviglia, Sci. Adv. **7**, eabf3096 (2021).
[21] P. Zhang, T.-F. Chung, Q. Li, S. Wang, Q. Wang, W. L. B. Huey, S. Yang, J. E. Goldberger, J. Yao, and X. Zhang, Nat. Mater. **21**, 1373 (2022).
[22] S. Li, L. Zhou, T. Frauenheim, and J. He, J. Phys. Chem. Lett. **13**, 6223 (2022).
[23] H. Ling and A. R. Davoyan, Nat. Photonics **16**, 259 (2022).

[24]B. Liu, S. Liu, L. Yang, Z. Chen, E. Zhang, Z. Li, J. Wu, X. Ruan, F. Xiu, W. Liu, L. He, R. Zhang, and Y. Xu, Phys. Rev. Lett. **125**, 267205 (2020).
[25]A. Barman, G. Gubbiotti, S. Ladak, A. O. Adeyeye, M. Krawczyk, J. Gräfe, C. Adelmann, S. Cotofana, A. Naeemi, V. I. Vasyuchka, B. Hillebrands, S. A. Nikitov, H. Yu, D. Grundler, A. V. Sadovnikov, A. A. Grachev, S. E. Sheshukova, J.-Y. Duquesne, M. Marangolo, G. Csaba, W. Porod, V. E. Demidov, S. Urazhdin, S. O. Demokritov, E. Albisetti, D. Petti, R. Bertacco, H. Schultheiss, V. V. Kruglyak, V. D. Poimanov, S. Sahoo, J. Sinha, H. Yang, M. Münzenberg, T. Moriyama, S. Mizukami, P. Landeros, R. A. Gallardo, G. Carlotti, J.-V. Kim, R. L. Stamps, R. E. Camley, B. Rana, Y. Otani, W. Yu, T. Yu, G. E. W. Bauer, C. Back, G. S. Uhrig, O. V. Dobrovolskiy, B. Budinska, H. Qin, S. van Dijken, A. V. Chumak, A. Khitun, D. E. Nikonov, I. A. Young, B. W. Zingsem, and M. Winklhofer, J. Phys.: Condens. Matter **33**, 413001 (2021).
[26]A. Hirohata, H. Sukegawa, H. Yanagihara, I. Zutic, T. Seki, S. Mizukami, and R. Swaminathan, IEEE Trans. Magn. **51**, 1 (2015).
[27]S. Y. Kim, T. Y. Kim, L. J. Sandilands, S. Sinn, M.-C. Lee, J. Son, S. Lee, K.-Y. Choi, W. Kim, B.-G. Park, C. Jeon, H.-D. Kim, C.-H. Park, J.-G. Park, S. J. Moon, and T. W. Noh, Phys. Rev. Lett. **120**, 136402 (2018).
[28]R. Galceran, B. Tian, J. Li, F. Bonell, M. Jamet, C. Vergnaud, A. Marty, J. H. García, J. F. Sierra, M. V. Costache, S. Roche, S. O. Valenzuela, A. Manchon, X. Zhang, and U. Schwingenschlögl, APL Mater. **9**, 100901 (2021).
[29]K. Hwangbo, Q. Zhang, Q. Jiang, Y. Wang, J. Fonseca, C. Wang, G. M. Diederich, D. R. Gamelin, D. Xiao, J.-H. Chu, W. Yao, and X. Xu, Nat. Nanotechnol. **16**, 655 (2021).
[30]E. Ressouche, M. Loire, V. Simonet, R. Ballou, A. Stunault, and A. Wildes, Phys. Rev. B **82**, 100408 (2010).
[31]H. Chu, C. J. Roh, J. O. Island, C. Li, S. Lee, J. Chen, J.-G. Park, A. F. Young, J. S. Lee, and D. Hsieh, Phys. Rev. Lett. **124**, 027601 (2020).
[32]U. F. P. Seifert, M. Ye, and L. Balents, Phys. Rev. B **105**, 155138 (2022).
[33]F. Wang, N. Mathur, A. N. Janes, H. Sheng, P. He, X. Zheng, P. Yu, A. J. DeRuiter, J. R. Schmidt, J. He, and S. Jin, Sci. Adv. **7**, eabj4086 (2021).
[34]E. Ergeçen, B. Ilyas, D. Mao, H. C. Po, M. B. Yilmaz, J. Kim, J.-G. Park, T. Senthil, and N. Gedik, Nat. Commun. **13**, 98 (2022).
[35]F. Mertens, D. Mönkebüscher, U. Parlak, C. Boix-Constant, S. Mañas-Valero, M. Matzer, R. Adhikari, A. Bonanni, E. Coronado, A. M. Kalashnikova, D. Bossini, and M. Cinchetti, Adv. Mater. **35**, 2208355 (2023).
[36]E. A. Mashkovich, K. A. Grishunin, R. M. Dubrovin, A. K. Zvezdin, R. V. Pisarev, and A. V. Kimel, Science **374**, 1608 (2021).
[37]T. Satoh, R. Iida, T. Higuchi, Y. Fujii, A. Koreeda, H. Ueda, T. Shimura, K. Kuroda, V. I. Butrim, and B. A. Ivanov, Nat. Commun. **8**, 638 (2017).
[38]Y. Suzuki, G. Hu, R. B. van Dover, and R. J. Cava, J. Magn. Magn. Mater. **191**, 1 (1999).
[39]F. Formisano, R. M. Dubrovin, R. V. Pisarev, A. M. Kalashnikova, and A. V. Kimel, J. Phys.: Condens. Matter **34**, 225801 (2022).
[40]C. Kim, J. Jeong, P. Park, T. Masuda, S. Asai, S. Itoh, H.-S. Kim, A. Wildes, and J.-G. Park, Phys. Rev. B **102**, 184429 (2020).
[41]C. Kim, H.-S. Kim, and J.-G. Park, J. Phys.: Condens. Matter **34**, 023001 (2022).
[42]G. Jackeli and G. Khaliullin, Phys. Rev. Lett. **102**, 017205 (2009).
[43]A. R. Wildes, V. Simonet, E. Ressouche, R. Ballou, and G. J. McIntyre, J. Phys.: Condens. Matter **29**, 455801 (2017).
[44]H. Zhang, Z. Ni, C. E. Stevens, A. Bai, F. Peiris, J. R. Hendrickson, L. Wu, and D. Jariwala, Nat. Photonics **16**, 311 (2022).
[45]E. J. K. B. Banda, Phys. Status Solidi **135**, K43 (1986).
[46]A. S. Borovik-Romanov, N. M. Kreĭnes, A. A. Pankov, and M. A. Talalaev, Sov. Phys.-JETP **37**, 890 (1973).
[47]T. W. J. Metzger, K. A. Grishunin, D. Afanasiev, R. M. Dubrovin, E. A. Mashkovich, R. V. Pisarev, and A. V. Kimel, Appl. Phys. Lett. **121**, 252403 (2022).
[48]G. A. Smolenskiĭ, R. V Pisarev, and I. G. Siniĭ, Sov. Phys. Uspekhi **18**, 410 (1975).
[49]J. Wagner, A. Sahasrabudhe, R. B. Versteeg, L. Wysocki, Z. Wang, V. Tsurkan, A. Loidl, D. I. Khomskii, H. Hedayat, and P. H. M. van Loosdrecht, Npj Quantum Mater. **7**, 28 (2022).
[50]J. Stöhr and S. Hans Christoph, *Magnetism* (Springer Berlin Heidelberg, Berlin, Heidelberg, 2006).
[51]M. F. Collins, *Magnetic Critical Scattering* (Oxford University Press Inc., New York, 1989).
[52]N. Tesařová, T. Ostatnický, V. Novák, K. Olejník, J. Šubrt, H. Reichlová, C. T. Ellis, A. Mukherjee, J. Lee, G. M. Sipahi, J. Sinova, J. Hamrle, T. Jungwirth, P. Němec, J. Černe, and K. Výborný, Phys. Rev. B **89**, 085203 (2014).
[53]A. V. Kimel, G. V. Astakhov, A. Kirilyuk, G. M. Schott, G. Karczewski, W. Ossau, G. Schmidt, L. W. Molenkamp, and T. Rasing, Phys. Rev. Lett. **94**, 227203 (2005).
[54]A. J. Kurtzig, R. Wolfe, R. C. LeCraw, and J. W. Nielsen, Appl. Phys. Lett. **14**, 350 (1969).
[55]J. R. Hortensius, D. Afanasiev, A. Sasani, E. Bousquet, and A. D. Caviglia, Npj Quantum Mater. **5**, 95 (2020).
[56]I. R. Jahn, Phys. Status Solidi **57**, 681 (1973).
[57]A. Kirilyuk, A. V. Kimel, and T. Rasing, Rev. Mod. Phys. **82**, 2731 (2010).
[58]A. V. Kimel, R. V. Pisarev, J. Hohlfeld, and T. Rasing, Phys. Rev. Lett. **89**, 287401 (2002).
[59]R. K. Pathria and P. D. Beale, *Statistical Mechanics* (Elsevier, 2011).
[60]Y. Takano, N. Arai, A. Arai, Y. Takahashi, K. Takase, and K. Sekizawa, J. Magn. Magn. Mater. **272–276**, E593 (2004).
[61]M. Pankratova, I. P. Miranda, D. Thonig, M. Pereiro, E. Sjöqvist, A. Delin, O. Eriksson, and A. Bergman, Phys. Rev. B **106**, 174407 (2022).
[62]S. Liu, A. Granados del Águila, D. Bhowmick, C. K. Gan, T. Thu Ha Do, M. A. Prosnikov, D. Sedmidubský, Z. Sofer, P. C. M. Christianen, P. Sengupta, and Q. Xiong, Phys. Rev. Lett. **127**, 097401 (2021).
[63]R. Merlin, Solid State Commun. **102**, 207 (1997).
[64]D. M. Juraschek and S. F. Maehrlein, Phys. Rev. B **97**, 174302 (2018).
[65]C. A. Belvin, E. Baldini, I. O. Ozel, D. Mao, H. C. Po, C. J. Allington, S. Son, B. H. Kim, J. Kim, I. Hwang, J. H. Kim, J.-G. Park, T. Senthil, and N. Gedik, Nat. Commun. **12**, 4837 (2021).
[66]A. S. Disa, M. Fechner, T. F. Nova, B. Liu, M. Först, D. Prabhakaran, P. G. Radaelli, and A. Cavalleri, Nat. Phys. **16**, 937 (2020).